Int. J. Electrochem. Sci., 9 **(2014)** 1715 - 1728

International Journal of
ELECTROCHEMICAL
SCIENCE
www.electrochemsci.org

Research on Corrosion Resistance of Electrodeposited CoPtP Film

Li Jiang[*], *Zhen Jin, Yi Sun, Panpan Wu, Qiujie Peng, , Guoying Wei, Hongliang Ge*

College of Materials Science and Engineering, China Jiliang University, Hangzhou, China
[*]E-mail: jiangliwhu@126.com

Received: 2 December 2013 / *Accepted:* 16 December 2013 / *Published:* 2 February 2014

In order to improve the corrosion resistance of CoPtP film in 3.5% NaCl solution, the effects of deposition current, temperature and perpendicular magnetic field (PMF) in the film preparation process were investigated. Results indicated that corrosion process of CoPtP film in 3.5% NaCl solution was controlled by cathodic process. At the condition of deposition current 0.08 A, temperature 60 ℃ and PMF intensity 0.5 T, the deposited film displayed good corrosion resistance and lowest corrosion current density 1.995×10^{-6} A/cm^2. The increase of deposition current, temperature and PMF intensity were beneficial to refine grains and enrich CoPx substances in CoPtP film. However, higher deposition current and temperature resulted in higher uneven stress and severer hydrogen evolution. Cracks on surface of films made corrosion resistance deteriorated.

Keywords: Electrodeposition; Perpendicular magnetic field; Corrosion; CoPtP film

1. INTRODUCTION

Recently cobalt-based magnetic thin films (CoW, CoPt, CoPtP, CoMoP, etc.) have been researched and applied in micro-electromechanical systems (MEMS) [1-9]. Electrodeposition is an attractive technique for shaped film fabrication, owing to its simplicity, low temperature and fast deposition rate. Cobalt (Co)-platinum (Pt) alloy has a high coercivity without high temperature annealing, since the Pt atom insert to the hcp structure of Co and result in a strong magnetic anisotropy. Small amount of P added into CoPt film can not only significantly increase the coercivity of film but also display some similar properties with the Co/Pt multilayer, such as strong perpendicular magnetic anisotropy, high coercive, and anti-oxidation [10].

The effect of magnetic field on film structure and magnetic performance has been researched in recent years [11]. Remsen [12] was the first to investigate the effect of magnetic field on the course of

chemical reactions and the effect of magnetic field on the electrode potential has been reported by Gross [13]. With the application of a permanent perpendicular magnetic field (PPMF) forces such as paramagnetic force (F_p), field gradient force (F_B), Lorentz force (F_L), electrokinetic force (F_E) and magnetic damping force(F_D) can become prominent in an electrode reaction [14]. Studies show that the magnetic field can affect bath property, film surface state, microstructure, alloy compositions and the crystal growth direction of electrocrystallization. Moreover, with the presence of magnetic field, Co electrodeposition rate is clearly enhanced due to an increase magnetic moment of Co^{2+} ions in solution influenced by the field gradient force and paramagnetic force. The CoPtP film deposited in magnetic filed with particular properties has been researched and reported in our lab [15, 16].

However, from the previous work of our research, it is found that if CoPtP film exposed to humid air at room temperature for several months, the bright film surface will be oxidized and lose metal luster. Corrosion of magnetic film in environmental conditions was usually an electrochemical process. For ample supply of oxygen and the presence of inorganic contaminants dissolved in the adsorbed water, an electrolyte was formed and enhanced the corrosion rates substantially. As the corrosion of CoPtP film carried out, the magnetic property weakened. Therefore, preparation CoPtP film with good corrosion resistance should be fully considerated during the deposition process.

The present study focus on the relationship of deposition conditions (deposition current, temperature and PMF intensity) and the corrosion resistance of CoPtP films, with the aim to provide longer service life of magnetic film applied in the fabrication of ULSI devices and MEMS.

2. MATERIALS AND METHODS

Electrodeposition of CoPtP films were performed in an alkaline bath. The components of the solution were summarized in detail in Table 1. Copper was used as the substrate, which was cut into 2×2 cm^2 with a diamond saw. A polish machine (MP-1A) was used to polish the surface of the copper. After the copper was polished, an alkaline solution (12 g/L NaOH, 60 g/L Na_2CO_3 and 60 g/L Na_3PO_4) was utilized to remove the oils in the copper surface. Then, the copper was dipped into H_2SO_4 (10%) solution to remove any oxides.

Table 1. Components and operating conditions of CoPtP film electrodeposition solution

Component	Concentration (mol/L)
$Co(NH_2SO_3)_2$	0.10
$Pt(NH_3)_2(NO_2)_2$	0.01
$NaH_2PO_2 \cdot H_2O$	0.06
$(NH_4)_2C_6H_6O_7$	0.20
NH_2CH_2COOH	0.10
Temperature (℃)	30-80
pH	8.0
Current (A)	0.06-0.1
Magnetic field (T)	0.1-0.5
Ultrasonic (W)	60

Finally, the substrate was immerged into 100 mL electrolyte to perform electrodeposition reaction for about 20 min. After the deposition was over, the CoPtP film was washed with a jet of deionized water and dried by a blower.

Electrochemical measurements, including potentiodynamic polarization curves and electrochemical impedance spectroscopy (EIS) were performed on electrochemical working station (PARSTAT®2273) with the conventional three electrode cell. The CoPtP film specimen was used as the working electrode, a platinum foil as counter electrode and a saturated calomel electrode (SCE) as reference electrode. The test solution was 3.5% NaCl aqueous solution. EIS was carried out at range of 10 mHz ~ 100 kHz with 5mV perturbation signal at the corrosion potential. To test the reliability and reproducibility of the measurements, duplicate experiments were performed. All tests are performed after the CoPtP film immersed in the 3.5% NaCl aqueous solution for 2 h.

Surface morphology of each specimen was observed using scanning electron microscopy (SEM, Hitachis-4800). And the microstructure was analyzed by X-ray diffractometer (XPert Philips PW1830) using a CuKα radiation as an incident beam at 40 kV and 150 mA.

3. RESULTS AND DISCUSSION

3.1 Influence of electrodeposition current

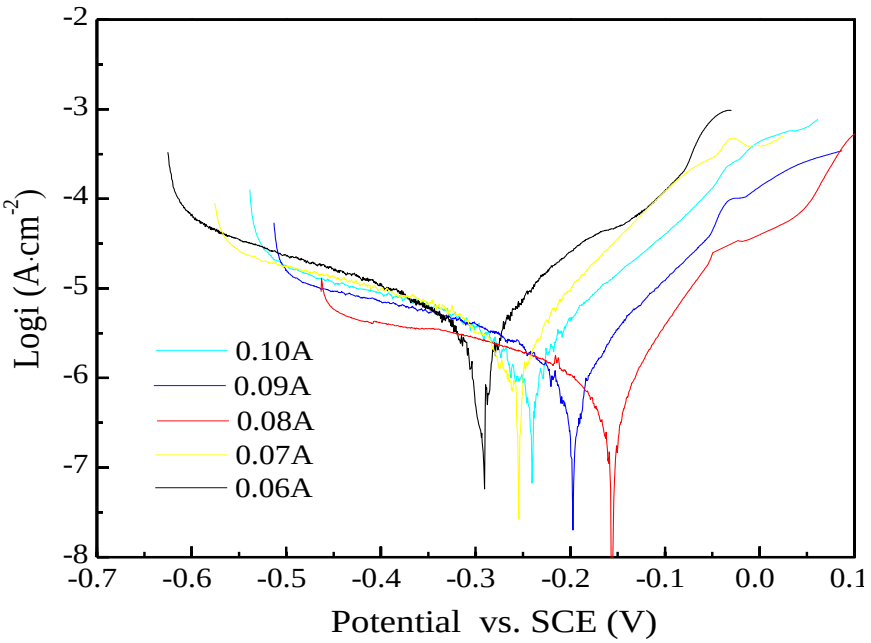

Figure 1. Polarization curves of CoPtP film prepared in solutions with different deposition currents (PMF 0.1 T, Temperature 50 ℃)

In electrodeposition process, the current destiny has a significant impact on the alloy composition and structure. According to diffusion theory, the metal electro-deposition rate has an upper limit. With the current density increased, deposition rate of metal with more negative potential

can be promoted, while deposition rate of metal with more positive potential is easier access to the limit [17]. Fig. 1 shows polarization curves of CoPtP films prepared in solutions with PMF 0.1 T, Temperature 50 ℃ and different deposition currents (0.06A-0.10A). The corrosion process of film in 3.5% NaCl solution is controlled by cathodic process. Corrosion current densities (I_{corr}) of films are calculated by Tafel extrapolation method shown in Table 2. Corrosion potential (E_{corr}) increases first and then decreases as deposition current value changes from 0.06 A to 0.10 A. CoPtP film displays best corrosion resistance with lowest corrosion current density 2.995×10^{-6} A/cm^2 at the preparation condition of deposition current 0.08 A.

Table 2. Corrosion current densities of CoPtP films prepared in solution with different deposition currents (PMF 0.1 T, Temperature 50 ℃)

Electrodeposition current(A) / Parameters	0.06	0.07	0.08	0.09	0.10
E_{corr} (V)	-0.291	-0.253	-0.156	-0.197	-0.248
I_{corr}(10^{-6}A/cm^2)	7.011	6.667	2.995	3.495	4.026

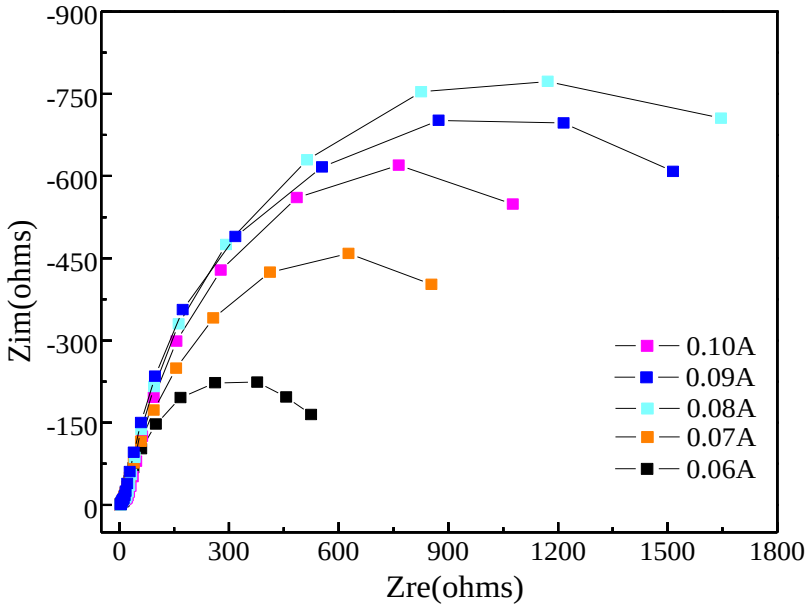

Figure 2. Nyquist plots of CoPtP films prepared in solution with different deposition currents (PMF 0.1 T, Temperature 50 ℃)

Nyquist plots of CoPtP films prepared in solution with different deposition currents are shown in Fig. 2. There is only one capacitive semicircle, which states one time constant in the Nyquist plot. In this study, R_t is only determined by the faradic process of the charge transfer controlled corrosion while R_f is affected simultaneously by charge transfer and mass transfer processes. The reciprocal of

the charge transfer resistance R_t is taken as a parameter to characterize the corrosion rate. As the deposition current increases, the charge transfer resistance R_t and surface film resistance R_f increase first and then decrease (see Table 3). When deposition current is 0.08 A, R_t and R_f are highest, exhibiting the best corrosion resistance of film in this experiment series.

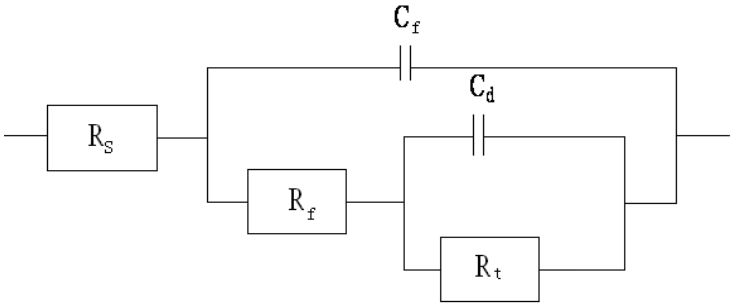

Figure 3. Equivalent circuit model of fitting EIS data (R_s is the solution resistance; C_f and R_f is the surface film capacitance and resistance; R_t is the charge transfer resistance; and C_d is the double layer capacitance.)

Table 3. Electrochemical parameters values of CoPtP films prepared in solution with different deposition currents (PMF 0.1 T, Temperature 50 ℃)

Deposition current(A) / Parameters	0.06	0.07	0.08	0.09	0.10
R_s (Ω)	4.092	4.018	4.197	4.018	4.041
C_f (μF)	2.72	2.24	2.13	2.23	1.93
R_f (Ω)	17.33	20.23	27.65	22.23	21.21
C_d (μF)	24.76	10.14	20.52	10.14	39.82
R_t (Ω)	569	1592	1668	1472	1232

Fig. 4 shows X-ray diffraction (XRD) patterns of the CoPtP films prepared in solution with different deposition currents. A diffractogram of the substrate shows a peak with high intensity at 2θ around 43.33°, which is due to copper with a preferred crystal orientation of [111]. Cobalt normally has a hexagonal structure at room temperature [18]. There are Co_2P (36.4° and 48.2°) and CoP_3 (72.8°) detected in the film. The increase of deposition current can enhance the deposition rate of metal with more negative potential. As the deposition current increases, content of these CoP substances (Co_2P and CoP_3) increase. However, the content of Pt_5P_2 (40.1°) in the film decreases slightly and CoPt (48.1°) changed little. The enrichment of Co and P elements in the film are beneficial to corrosion resistance enhancement [19-21]. The Co substance can make the film structure denser by forming cobalt oxide or passive film, which prevented the penetration of external corrosion factors and reduced the release of metal ions [19, 20]. The possible segregation of P in the grain boundaries or the enrichment of P on the surface seems to minimize the corrosion process of the film [21].

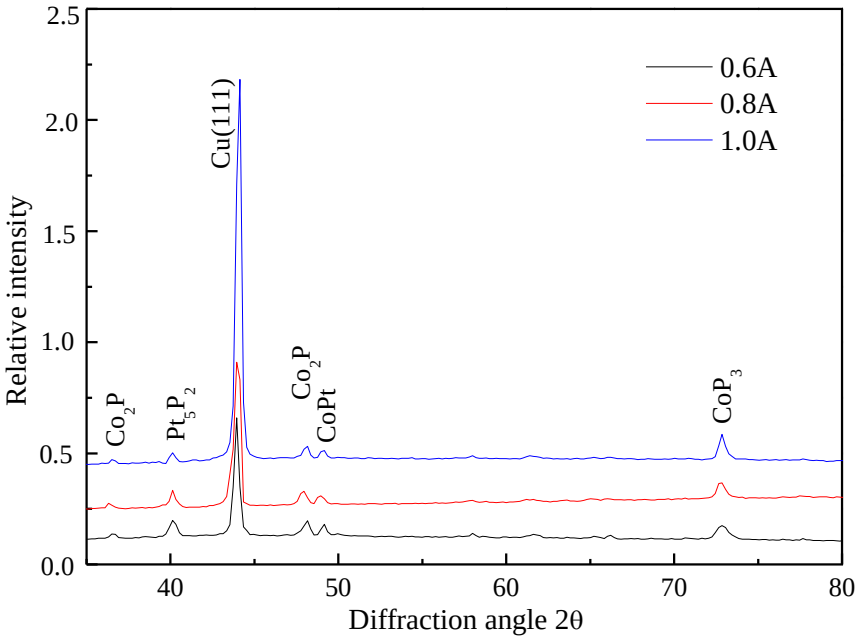

Figure 4. XRD patterns of CoPtP films prepared in solutions with different deposition currents (PMF 0.1 T, Temperature 50 ℃)

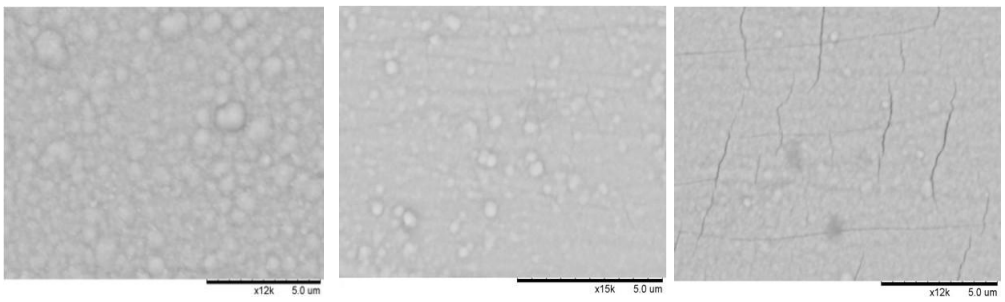

(a) 0.06 A (b) 0.08 A (c) 0.10 A

Figure 5. Surface morphology of CoPtP films prepared in solution with different deposition currents (a) 0.06 A; (b) 0.08 A; (c) 0.10 A (PMF 0.1 T, Temperature 50 ℃)

Fig. 5 shows the surface morphology of CoPtP films prepared in solution with different deposition currents. The lower deposition current results in lower deposition rate of film. When deposition current is 0.06 A, grains on film are relatively sparse and uneven distribution. Fast deposition current apt to promote reaction and deposition rates, and result in more grains generating on surface of film with smaller size. According to the results of XRD shown in Fig. 4, the average grain sizes of crystalline films can be calculated using the Debye-Scherrer equation [22]:

$$D = k\lambda/(\beta\cos\theta) \quad (1)$$

Where D is the grain size, K is the Scherrer constant, λ is the wavelength of X-ray and β is the diffraction angle. As the deposition current increases, grain sizes decreases: 64-78 nm (deposition current 0.06 A), 57-69 nm (deposition current 0.08 A) and 45-62 nm (deposition current 0.10 A)

respectively. However, since the increase of uneven stress generated in the deposition process, full of cracks emerged on the film deposited with current 0.10 A. It is in favor of the wicked environmental factors such as Cl^- penetrated through cracks and caused substrate corrosion. This phenomenon is the same with that detailed in Meritxell's study [21]. It is the reason that corrosion resistance of film deposited with current 0.10 A is worse than that of film deposited with current 0.08 A.

3.2 Influence of deposition temperature

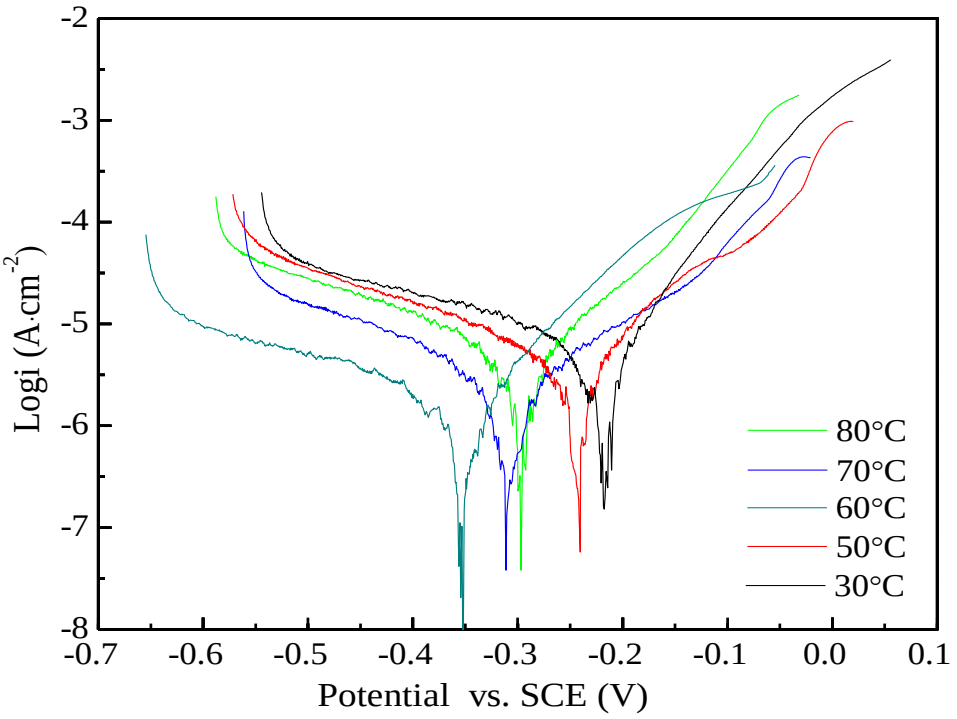

Figure 6. Polarization curves of CoPtP film prepared in solution with different deposition temperatures (PMF 0.1 T, Current 0.08 A)

Table 4. Corrosion potential and current of CoPtP film prepared in solutions with different deposition temperatures (PMF 0.1 T, Current 0.08 A)

Temperature (℃) / Parameters	30	50	60	70	80
E_{corr} (V)	-0.225	-0.242	-0.352	-0.312	-0.301
I_{corr}(10^{-6}A/cm^2)	6.981	6.309	2.365	3.162	5.011

The polarization curves of CoPtP film prepared in solution under different deposition temperatures are shown in Fig. 6. Corrosion potentials and currents are calculated by Tafel extrapolation method shown in Table 4. As the deposition temperature increases from 30 ℃ to 60 ℃,

potentials of CoPtP film in 3.5% NaCl solution moved to the negative direction, and corrosion current is the lowest 2.365×10^{-6} A/cm^2. While as the deposition temperature increases from 60 ℃ to 80 ℃, the change rules of potential and corrosion rate are the opposite, that is, corrosion potential moves of the positive direction and corrosion rate increases. Therefore, the deposition temperature 60 ℃ is the proper parameter in the preparation of CoPtP film.

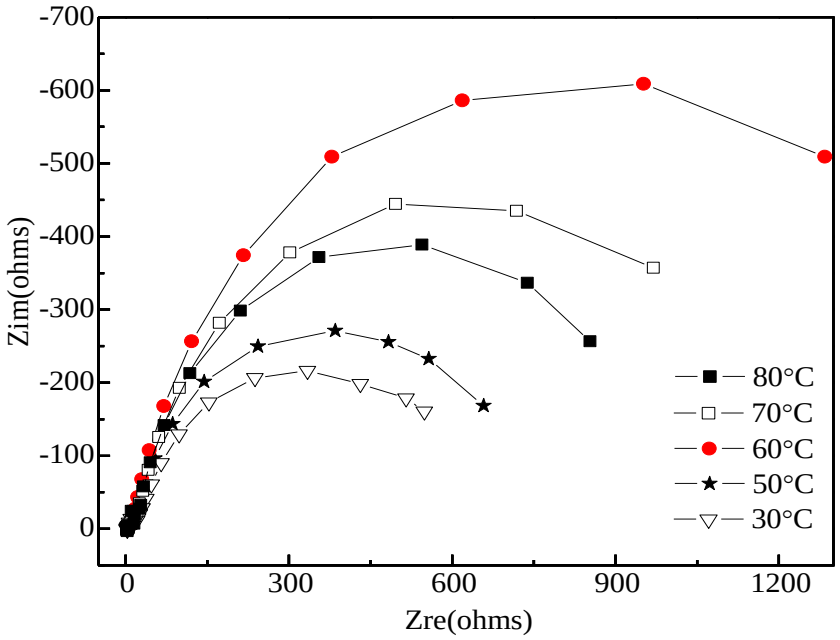

Figure 7. Nyquist plots of CoPtP film prepared in solution with different deposition temperatures (PMF 0.1 T, Current 0.08 A)

Table 5. Electrochemical parameters values of CoPtP films prepared in solution with different deposition temperatures (PMF 0.1 T, Current 0.08 A)

Temperature (℃) / Parameters	30	50	60	70	80
R_s (Ω)	3.574	3.854	4.102	3.274	3.707
C_f (μF)	4.72	3.11	6.892	1.02	1.65
R_f (Ω)	22.371	24.44	27.88	26.75	25.65
C_d (μF)	25.71	25.30	35.25	33.23	28.90
R_t (Ω)	525.7	564.3	898.1	823.1	788.3

Fig. 7 shows Nyquist plots of CoPtP films prepared in solution with PMF 0.1T, deposition current 0.08A and different deposition temperatures (30-80℃). It reveals the change regulation of membrane and charge transfer resistances, membrane and double layer capacitances. The equivalent circuit model of fitting EIS data are the same with that shown in Fig. 3. Table 5 presents

electrochemical parameters values of CoPtP films prepared in solutions with different deposition temperatures. As the deposition temperature increases from 30 ℃ to 80 ℃, surface film resistance R_f and charge transfer resistance R_t increase first and then decrease. When deposition temperature is 60 ℃, R_f and R_t reach to the highest values and the film displays better corrosion resistance.

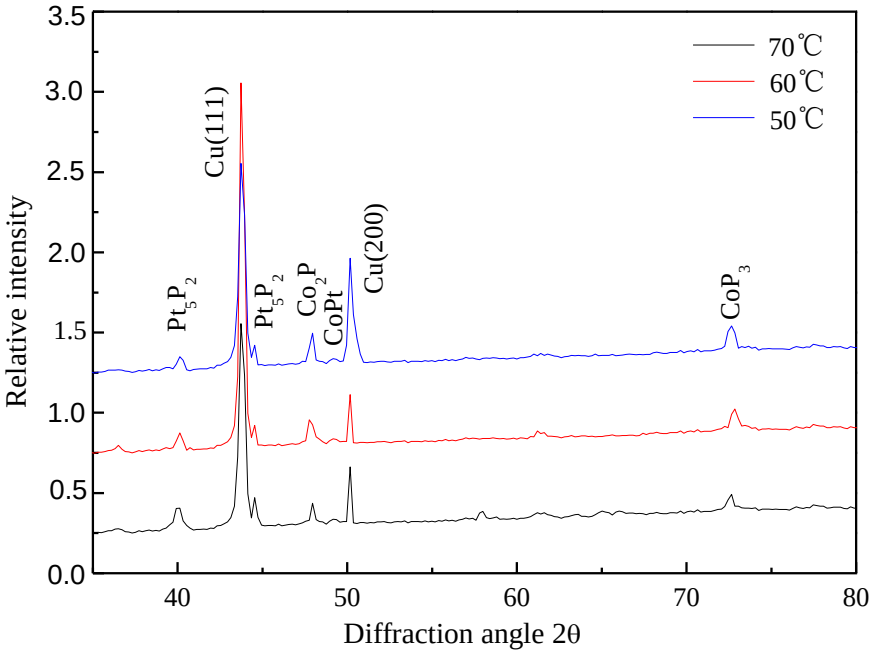

Figure 8. XRD patterns of CoPtP films prepared in solution with different deposition temperatures (PMF 0.1 T, Current 0.08 A)

Fig. 8 shows the XRD patterns of CoPtP films prepared in solution with different deposition temperatures. The strong peaks at 43° and 50° demonstrates the (111) and (002) texture of basement Cu. As the deposition temperature increases, contents of substance CoP_3 and Co_2P increase, while Pt_5P_2 decreases slightly. The rise of deposition temperature has little effect on content of CoPt. This change rules are same with that of deposition current.

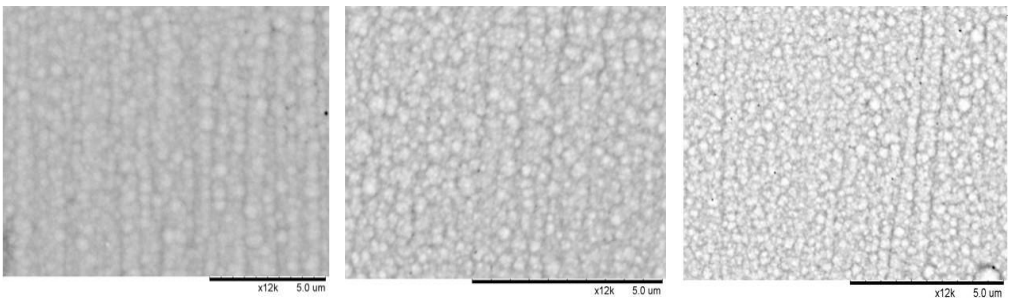

(a) 50 ℃ (b) 60 ℃ (c) 70 ℃

Figure 9. Surface morphology of CoPtP films prepared in solution with different deposition temperatures (a) 50 ℃; (b)60 ℃; (c)70 ℃ (PMF 0.1 T, Current 0.08 A)

Fig. 9 shows the surface morphology of CoPtP films prepared in solution with different deposition temperatures. As the increase of deposition temperature, film become compact and uniform gradually. According to the results of XRD shown in Fig. 8, the average grain sizes of crystalline films are calculated using the Debye-Scherrer equation. When deposition temperature is 60 ℃, the film surface was uniformity with moderate grain sizes (55-67nm). Finer grains (44-59nm) are obtained when deposition temperature is 70 ℃. In the process of electrodeposition, electrolyte temperature has a significant impact on the deposition rate of film. Within a suitable range for plating, the increase of temperature can promote the deposition rate of film, e.g. if the deposition temperature increases 10 degree, the deposition rate increased from 2 to 4 times [17]. Higher deposition temperature may lead to fast reaction rate, and give rise to obvious effect of hydrogen [23]. When deposition temperature was 70 ℃, many small cracks emerge on the film surface and result in deterioration of corrosion resistance.

3.3 Influence of perpendicular magnetic field (PMF)

Since cobalt is a ferromagntetic element, in magnetic field, the magnetizing force will affect the deposition of CoPtP film. Lorentz force makes the charged particles do spiral movement in the magnetic field and finally get to the cathode surface sideways. The tangential movements of ions near the cathode make the diffusion layer thinner, which can stir the bath, improve the mass transfer rate and reduce the concentration polarization of electrode surface [24]. Magnetizing force can make some changes on film magnetic performance, surface morphology and corrosion resistance [25].

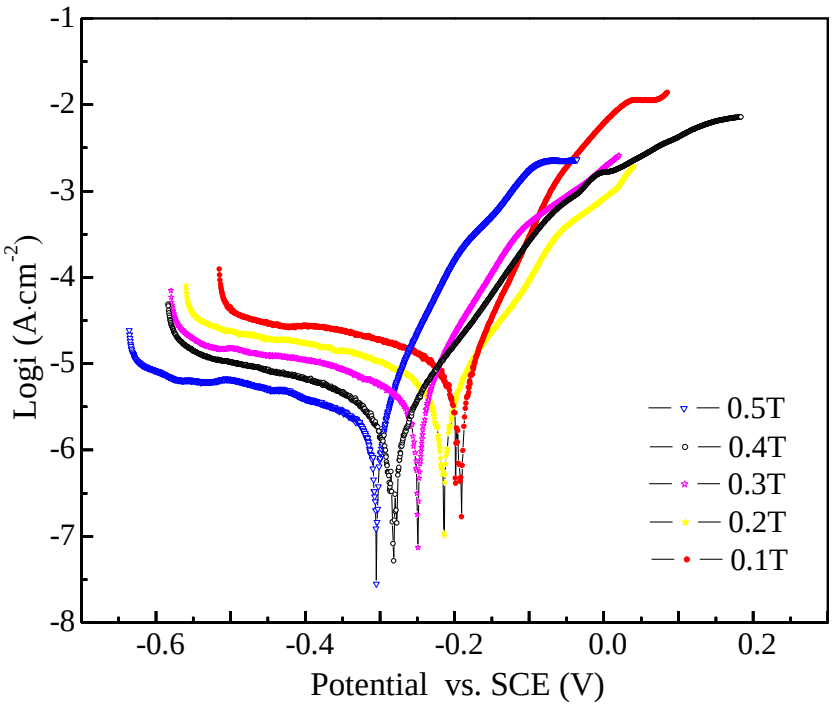

Figure 10. Polarization curves of CoPtP film prepared in solution with different PMFs (Current 0.08 A, Temperature 60 ℃)

Polarization curves of CoPtP film prepared in solution with deposition current 0.08 A, temperature 60 ℃ and different PMFs (0.1-0.5 T) are shown in Fig. 10. The corrosion process controlled by cathodic reaction can be seen obviously. Corrosion potentials and currents are calculated by Tafel extrapolation method and shown in Table 6. As the PMF intensity increases from 0.1 T to 0.5 T, corrosion potential of film has a trend of negative movement and the corrosion current density decreases from 8.913×10^{-6} A/cm^2 to 1.995×10^{-6} A/cm^2.

Table 6. Corrosion potential and current of CoPtP films prepared in solution with different PMFs (Current 0.08 A, Temperature 60 ℃)

PMF(T) / Parameters	0.1	0.2	0.3	0.4	0.5
E_{corr} (V)	-0.191	-0.214	-0.249	-0.281	-0.305
I_{corr} (10^{-6}A/cm^2)	8.913	7.709	4.169	3.162	1.995

Nyquist plots for CoPtP films deposited with different PMFs in 3.5%NaCl solution for 2 h are shown in Fig. 11. The general trend of the impedance measurements is in agreement with expectation. The impedance spectra of the Nyquist plots are analyzed by fitting to the equivalent circuit model shown in Fig. 3. As PMF intensity increases, the double layer capacitance C_d declines, which indicate that it is influenced by the state of electrode/solution interface and the real contact area between electrode and solution; while the surface film resistance R_f increases from 14.9 Ω to 78.71Ω and charge transfer resistance R_t increases from 466.0 Ω to 1147.0 Ω (shown in Table 7). These changes demonstrate that the modified CoPtP film influenced by PMF is denser and compact, as well as, has better property against the penetration of external corrosion factors.

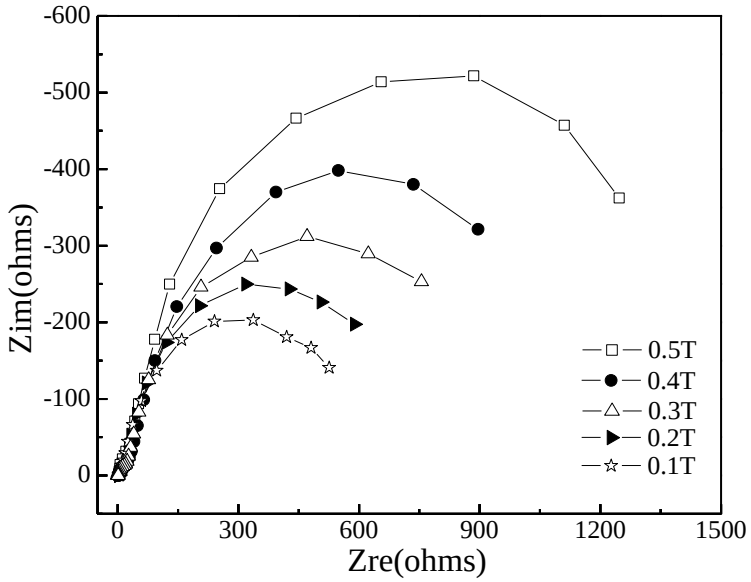

Figure 11. Nyquist plots of CoPtP film prepared in solution with different PMFs (Current 0.08 A, Temperature 60 ℃)

Table 7. Electrochemical Parameters values of CoPtP film prepared in electroplating solutions with different PMFs (Current 0.08 A, Temperature 60 ℃)

PMF (T) / Parameters	0.1	0.2	0.3	0.4	0.5
R_s (Ω)	3.296	3.253	3.0947	2.571	2.171
C_f (μF)	4.141	2.425	2.117	2.236	2.361
R_f (Ω)	14.9	19.51	28.05	35.27	78.71
C_d (μF)	21.25	33.83	34.53	29.49	15.25
R_t (Ω)	466	545.3	677.6	832.1	1147

The structures of CoPtP films prepared in solution with different PMFs analyzed by XRD are shown in Fig. 12. Co was a ferromagnetic metal and then the trajectory of Co ions will be changed by the obvious effects of field gradient force, electric field force and Lorentz force in the PMFs. Co ions are driven to reach the cathode surface earlier and proceeded reduction reactions. The effects of PMF on Pt-substance are not obvious. Therefore, as the PMFs intensity increase, the content of Co_2P, CoPt and CoP_2 increased.

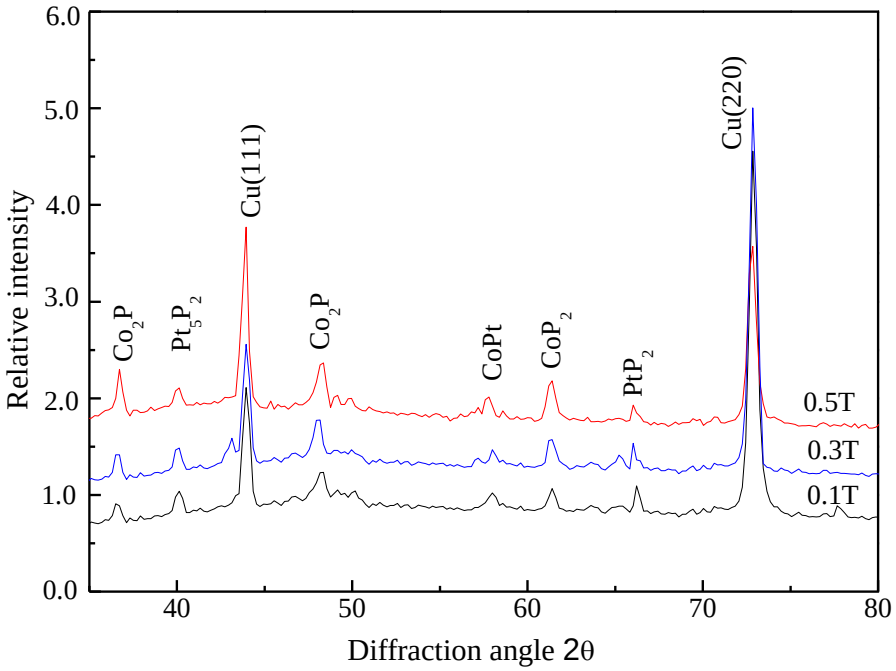

Figure 12. XRD pattern of CoPtP films prepared in solutions with different PMFs (Current 0.08 A, Temperature 60 ℃)

PMF applied in the deposition process of CoPtP film can change the precipitation mode and the film morphology. The morphology of CoPtP films deposited under different PMF is shown in Fig. 13. According to the results of XRD shown in Fig. 12, the average grain sizes of crystalline films are

calculated. The grains formed in PMF 0.1 T are large (72-89 nm) and some little voids are formed. As the intensity of PMF increases, it is very conspicuous to observe that the grains size become smaller (0.3 T, 62-83 nm; 0.5 T 53-69 nm), the film surface appeared compactly. Moreover, the holes affected by hydrogen evolution reaction on the surface disappeared gradually.

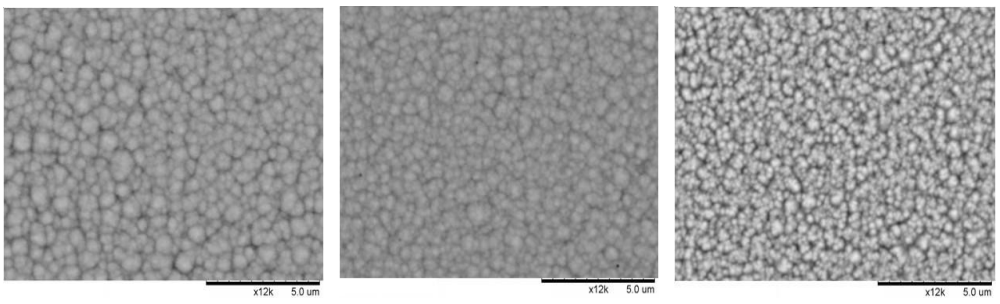

(a) 0.1 T (b) 0.3 T (c) 0.5 T

Figure 13. Surface morphology of CoPtP films prepared in solutions with different PMFs (a) 0.1 T; (b) 0.3 T; (c) 0.5 T (Current 0.08 A, Temperature 60 ℃)

The reason is that [26] the existed PMF restrains the convection and diffusion of ions in electrolyte, thus the diffusion of ions reduced and the structure of deposits refined.

4. CONCLUSIONS

In this paper, effects of deposition conditions on CoPtP film's corrosion resistance in 3.5% NaCl solution were discussed, and some optimal parameters of deposition were obtained. At the condition of deposition current 0.08 A, temperature 60 ℃ and PMF intensity 0.5 T, the deposited film displayed good corrosion resistance and lowest corrosion current density 1.995×10^{-6} A/cm^2. The increase of deposition current, temperature and PMF intensity were beneficial to refine grains and promote the contents of CoPx substances in CoPtP film. The enrichment of Co and P elements in the film can enhance its corrosion resistance. However, since the cracks resulted by uneven stress and hydrogen separation, corrosion resistance of film deteriorated.

ACKNOWLEDGEMENT
This research was supported by funds from the National Science Foundation of China (No.20971116 and No.21171155), International Scientific and Technological Cooperation Project (No.2011DFA52400), the Natural Science Foundation of Zhejiang Province (No. LQ12E01005) and Students Research and Innovation Team Project of Zhejiang Province (No. 2013R409026).

References

1. E. Rudnik, M. Mucha, *Surf. Eng.*, 27(2011)683.
2. Y. Shacham-Diamand, A. Inberg, Y. Sverdlov, V.Bogush, N. Croitoru, H. Moscovich and A. Freeman, *Electrochim. Acta*, 48(2003)2987.

3. V. Dubin, Y. ShachamDiamand and B. Zhao, *J. Electrochem. Soc.*, 144(1997)898.
4. P. C.Andricacos, C. Uzoh and J. O. Dukovic, *IBM J. Res. Dev.*, 42(1998)567.
5. A. Kohn, M. Eizenberg and D. Y. Shacham, *Mater. Sci. Eng. A*, 302(2009)18.
6. M. Paunovic, P. J. Bailey and R. G. Schad, *J. Electrochem. Soc.*, 141(2004)1843.
7. Y. Shacham-Diamand and S. Lopatin, *Electrochim. Acta*, 44(1999)3639.
8. Y. Shacham-Diamand, *J. Electron. Mater.*, 30(2010)336.
9. Y. Shacham-Diamand, Y. Sverdlov and N. Petrov, *J. Electrochem. Soc.*, 148(2010) C162.
10. C. Fowley, Z. Diao and C. C. Faulkner, *J. Phys. D: Appl. Phys.*, 46(2013) 195501.
11. L.Jiang, J.B.Lu,S.S.Pan, Y. D. Yu, G.Y. Wei and H. L. Ge, *Int. J. Electrochem. Sci.*, 7(2012) 2188.
12. J. Remsen, *Lumiere. Electr.*, 10 (1888) 468.
13. A. Gross, *Vien. Ber.*, 92(1885)1378.
14. G. Hinds, J. M. D. Coey and M.E.G. Lyons, *Electrochem. Comm.*, 10 (2001)3215.
15. Y.D. Yu, W. Li, J.W. Lou, H.L. Ge, L.X. Sun, L. Jiang and G. Y. Wei, *Rare metals*, 31(2012)125.
16. Y.D. Yu, J.W. Lou, W. Li, L.X. Sun, H.L. Ge and G. Y. Wei, *Mater. Sci. Technol.*, 28 (2012)448.
17. G. Wang, X.L. Ling and F. Xiao, *Opt. Laser Technol.*, 49(2013)274.
18. Y. D. Yu, H.F. Guo, J.W. Lou, H.L. Ge and G. Y. Wei, *Mater. Res. Innovations*, 16(2012)179.
19. X.P. Xiao, H.Y. Xu and J. Liu, *Plat. Surf. Finish*, 32(2010)202.
20. S.F. Shi, J. Lin and B. Zhou, *Rare Met. Mater. Eng.*, 36(2007)37.
21. C. Meritxell, G. Elvira and V. Elisa, *J. solid state Electrochem.*, 14(2010)2225.
22. Y.D. Yu, G.Y. Wei and H.L. Ge, *Surf. Rev. lett.*, 16(2009)635.
23. X. Qiao, H. Li and W. Zhao, *Electrochim. Acta*, 89(2013)771.
24. C. Takashi, A. Jun and H. Naoki, *J. Magn. Magn. Mater.*, 287(2005)167.
25. N. Yoshihisa, *J. Magn. Magn. Mater.*, 200(1999)634.
26. K. H. Lee, J. Yoo, J. Ko and H. Kim, *Phys. C*, 372(2002)866.